

## MICROWAVE ELECTRODYNAMICS

---

# Slot Resonances in Axially Symmetric Radiators of Pulse-Modulated and Monochromatic $TM_{0n}$ -modes\*

*K.Yu. Sirenko*

A. Usikov Institute of Radio Physics and Electronics,  
National Academy of Sciences of Ukraine  
12, Academician Proskura St., Kharkiv 61085, Ukraine

**ABSTRACT:** The resonances of  $TEM$  -modes supported by narrow radial and coaxial circular waveguides are analyzed. By exciting such resonances it should be possible to effectively control the electrodynamic characteristics of classical axially-symmetric radiators.

Owing to the simple design of axially-symmetric waveguiding elements and radiators, they can be easily integrated into electrodynamic systems of various application. A number of special technologies have existed and constantly revised that permit of quick and low cost manufacturing of such devices (see, for example, paper [1]). The spectrum of operational modes of practical interest pertaining to such structures can be greatly extended through excitation therein of slot resonances. Specifically, this concerns  $TEM$  -mode resonances in radial and circular waveguides which change only slightly the general geometry of classical electrodynamic units.

The slot resonances and their role in forming the response of axially-symmetric waveguiding units to pulse-modulated or monochromatic  $TM_{0n}$  driving modes were first considered in paper [2]. In the present paper slot resonances are analyzed that arise as a result of slight changes in the geometry of the simple axially-symmetric radiators. These geometries are represented by the section of a circular coaxial waveguide with a thick external wall protruding over the flange (Fig. 1(a)) and the cylindrical monopole extension to the central conductor of a coaxial feed line (Fig. 2(a)).

---

\* Originally published in *Radiophysics and Electronics*, Vol. 11, No 2, 2006, pp. 196-204.

All the results presented have been obtained by the methods described in detail in papers [3,4]. The methods are based on the equivalent replacement of model “open” initial and boundary value problems of the non-sinusoidal wave dynamics by “closed” ones, with application of the standard finite-difference [5]. The transition to the “closed” problems is performed using original exact “absorbing” conditions whose application at the virtual boundaries of the analyzed domains does not distort the physics of the modeled processes of pulse-modulated electromagnetic wave propagation and scattering.

The reliability and efficiency of the approach have been confirmed by analyzing a set of special test problems (see an example in paper [6]). In particular, the pulsed response of a conic monopole has been reproduced in every detail. Prior to that, the monopole serving as an extension to the central conductor of a coaxial feed line was analyzed numerically and measured experimentally in paper [7].

## SIMPLE AXIALLY-SYMMETRIC ANTENNAS

Geometries and basic electrodynamic characteristics of classical axially-symmetric ( $\partial/\partial\phi=0$ ) structures are shown in Figs. 1 (antenna 1) and 2 (antenna 2). The source geometries are presented in these Figures as cross-sections by the half-plane  $\phi = \pi/2$ ; the axis of symmetry of the radiator coincides with the  $z$ -axis; the flanges are infinite within the plane  $z = 0$ ; and  $a$  and  $b$  are, respectively, the radii of the internal and external conductors of the feeding semi-infinite coaxial waveguides if circular cross-section.

Here

$$D(\vartheta, k, M) = \frac{|\tilde{E}_\vartheta(M, \vartheta, k)|^2}{\max_{0 < \vartheta < \pi/2} |\tilde{E}_\vartheta(M, \vartheta, k)|^2}$$

is the normalized power pattern of the antenna, taken at a fixed radius  $r = M$ ;  $0 \leq \vartheta \leq 90^\circ$ ;  $\tilde{E}_\vartheta(r, \vartheta, k)$  are spectral amplitudes of the  $E_\vartheta(r, \vartheta, t)$ - component of the electromagnetic field of Eq. (1);  $k = 2\pi/\lambda$  is the wavenumber (also, the frequency parameter or simply the frequency);  $\lambda$  is the free-space wavelength;  $\bar{\vartheta}(k)$  is the orientation angle of the main lobe of the antenna pattern;  $\eta(k)$  is the radiation efficiency (i.e., the portion of the delivered power which is radiated into free space); and  $\rho, \phi, z$  and  $r, \vartheta, \phi$  are the cylindrical and spherical polar coordinated, respectively.

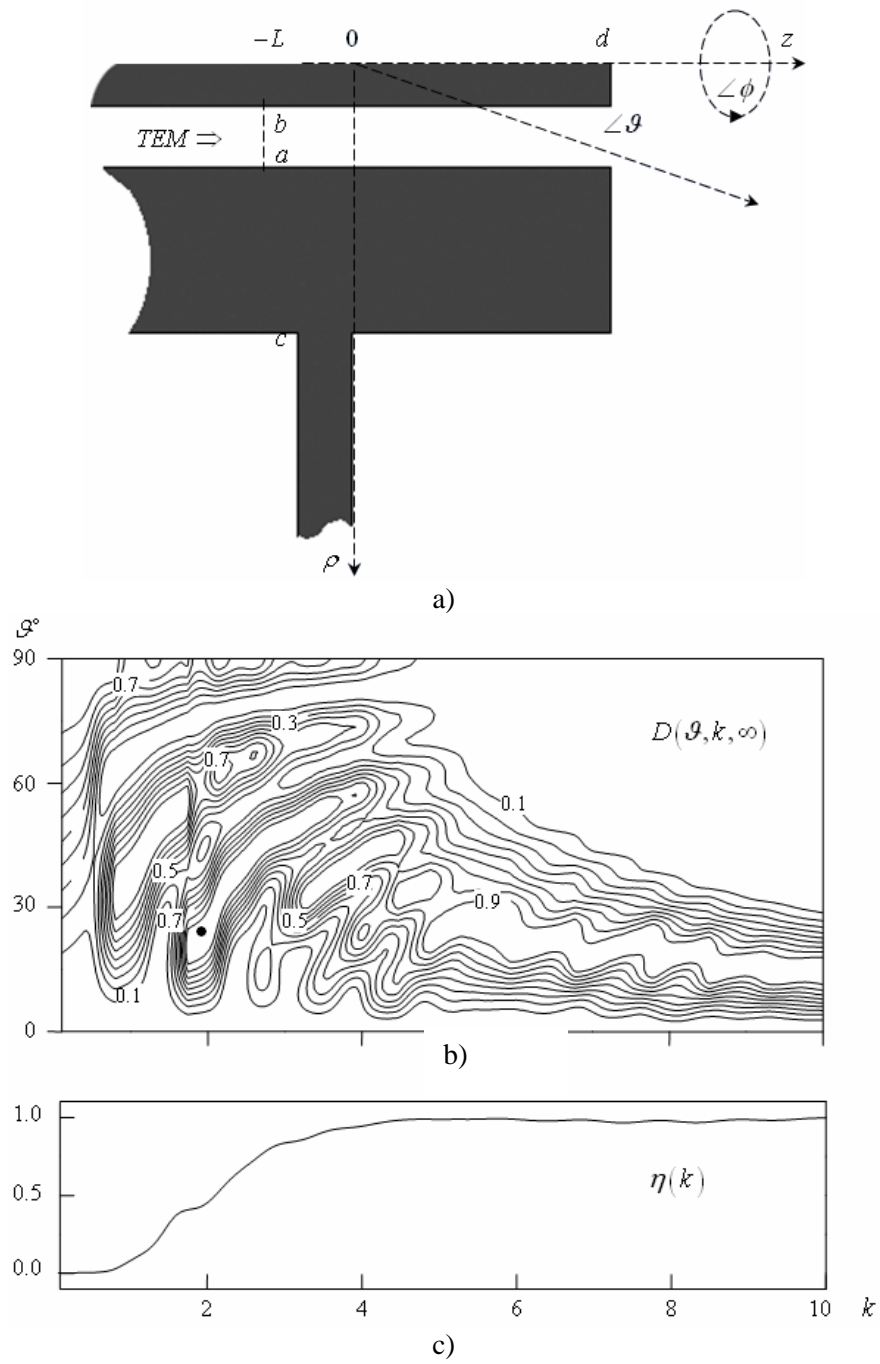


**FIGURE 1.** Antenna 1: (a) geometry of the antenna ( $a = 1; b = 0.4; c = 2.6; d = 2.5; L = 0.5$ ); (b) antenna pattern, and (c) radiation efficiency

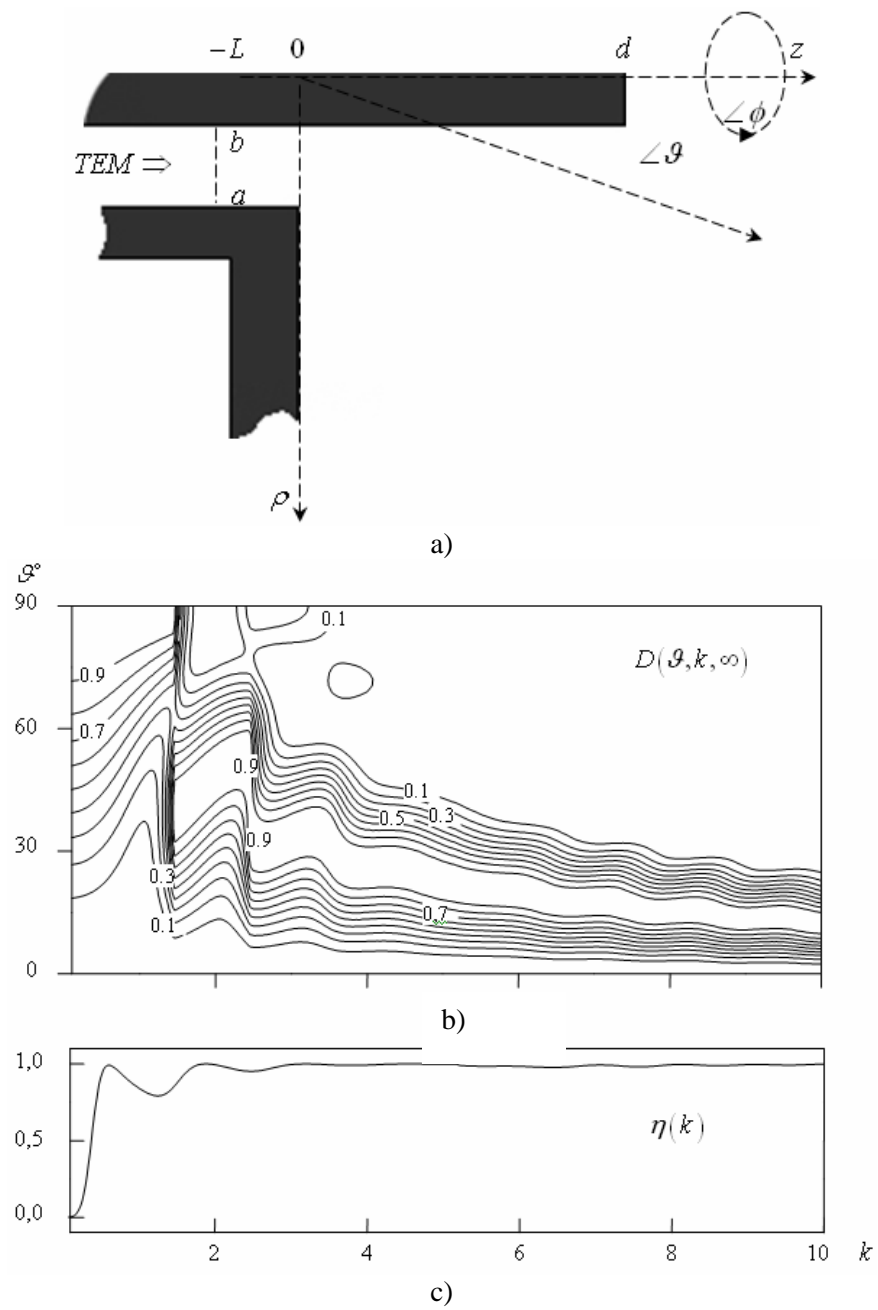


**FIGURE 2.** Antenna 2: (a) antenna geometry ( $a = 1; b = 0.4; d = 2.5; L = 0.5$ ); (b) antenna pattern, and (c) radiation efficiency

The frequency responses  $\tilde{f}(k)$  can be obtained from the temporal characteristics  $f(t)$  using the Fourier transformation, viz.

$$\tilde{f}(k) = \frac{1}{2\pi} \int_0^T f(t) e^{ikt} dt \leftrightarrow f(t) = \int_{-\infty}^{\infty} \tilde{f}(k) e^{-ikt} dk, \quad (1)$$

where  $T$  is the length of the observation interval  $t \in [0; T]$ .

The dimensions of all the physical values are in conformity with the International System of units (SI), whereas the time  $t$  is measured in meters, being in fact a product of the real time and the free-space velocity of light.

The antennas are excited by a super-wideband *TEM* pulse through the virtual boundary  $z = -L$  set within the transverse cross-section of the feeding coaxial waveguide. The amplitude of the pulse  $E_\rho$ -component is given by the expression

$$v_0^\rho(-L, t) = A \frac{\sin[\Delta k(t - \tilde{T})]}{(t - \tilde{T})} \cos[\tilde{k}(t - \tilde{T})] \chi(t - T),$$

with  $\tilde{k} = 5.5$ ;  $\Delta k = 5.5$ ;  $A = 4$ ;  $\tilde{T} = 25$ ;  $T = 130$ , and  $\chi$  is the Heaviside step function. Such a source illuminates uniformly the scanned frequency range  $0.1 \leq k \leq 10$ . The feeding waveguide operates as a single-mode structure at the lower frequency end of the range ( $k < k_1 \approx 5.18$ ;  $k_n$  being the cutoff point for the  $TM_{0n}$ -wave), and a dual-mode waveguide at higher frequencies ( $k < k_2 \approx 10.44$ ).

If a more detailed analysis of the source properties is required within a narrow frequency band, then the amplitude of the  $E_\rho$ -component is given by

$$v_0^\rho(-L, t) = \cos[\tilde{k}(t - \tilde{T})] P(t), \quad (2)$$

where  $\tilde{k}$  is the central frequency;  $\tilde{T} = 0.5$ , and  $P(t)$  is a trapezoidal envelope equal to zero at  $t < 0.01$  and  $t > 90$ , and equal to one over the interval  $5 < t < 85$ .

Among the essential features of the simple radiation sources under analysis note the following:

The radiation efficiency,  $\eta(k)$ , of antenna 1 grows from zero to one as  $k$  is increased (in the vicinity of the point  $k = k_1$ ), and further on drops off only slightly from its maximum level. The two first sharp changes in the orientation  $\bar{\vartheta}(k)$  of the main lobe of the antenna pattern (reorientation of the antenna pattern) occur at  $\lambda \approx 2(d + c - a)$  and  $\lambda \approx d + c - a$ , respectively.

The radiation efficiency,  $\eta(k)$ , of antenna 2 shows a monotonous increase from zero to  $\bar{\eta}_1 \approx 1$  within the range  $0 < k < \bar{K}_1$ . The function  $\eta(k)$  attains its first local maximum,  $\bar{\eta}_1$ , at the point  $k = \bar{K}_1$  for which  $\lambda \approx 4d$ . The second maximum,  $\bar{\eta}_2$ , occurs at the point  $k = \bar{K}_2$  where  $3\lambda \approx 4d$  (both are quarter-wave resonances).

The first local minimum,  $\underline{\eta}_1$ , of the function  $\eta(k)$  is attained at the point  $k = \underline{K}_1$  for which  $\lambda \approx 2d$ , while the second one,  $\underline{\eta}_2$ , at the point  $k = \underline{K}_2$  for which  $\lambda \approx d$  (half-wave resonances).

The function  $D(\vartheta, k)$  changes sharply near the point  $k = \underline{K}_1$  and  $k = \underline{K}_2$ . Specifically, the main lobe of the antenna pattern here becomes narrower and closer to the  $z$ -axis.

At longer wavelengths,  $0 < k < \underline{K}_1$ , the radiated  $TM_0$ -wave propagates perpendicularly to the structure axis of symmetry.

At greater values of  $k$  the function  $\eta(k)$  is close to one, which the antenna pattern shows slight monotonous changes. The main lobe of the pattern slowly grows thinner, gradually approaching the orientation angle  $\bar{\vartheta}(k) \approx 14^\circ$ .

## SLOT RESONANCES IN ANTENNA 1

A thin radial slot in the external conductor of antenna 1 (see Figs. 3(a) and 3(c) where the slot is divided by the plane  $z = 2$  into two equal parts; the slot width is 0.06) allows increasing essentially the radiation efficiency in the vicinity of the point  $\bar{k} = 1.91$  ( $\eta(\bar{k}) \approx 1$ ,  $\bar{\lambda} = 2\pi/\bar{k} = 3.3 \approx 2(c - a)$ ) long before the propagational  $TM_{01}$ -wave appears in the feed line. Qualitatively, the radiation pattern outside this vicinity changes only slightly, while its main lobe is reoriented from the direction  $\bar{\vartheta} \approx 24^\circ$  to  $\bar{\vartheta} \approx 55^\circ$  (Fig. 1(b): the heavy dot corresponds to the value  $D(24^\circ, 1.91, \infty) = 1$ ).

The appearance of a half-wave resonance for the  $TEM$ -wave in the slot a narrow radial waveguide does not always result in increasing the radiation efficiency of the antenna to  $\eta = 1$ . It is also necessary to match the resonance wavelength with the spatial phase of the  $TEM$  mode in the coaxial feed line on its way from the slot to the aperture and back, and the feed line itself should be a single-mode one. Under these conditions even a completely closed aperture does not impede the fed power to be radiated efficiently into free space (see Figs.3(b) and 3(d): the short plug is located within the plane  $z = 2 + 1.65 = 3.65$ ; the distance from the slot the short plug is equal to one half of the resonant wavelength;  $\eta(\bar{k}) \approx 1$  for frequencies close to  $\bar{k}$ , and  $\bar{\vartheta} \approx 45^\circ$ ).

A narrow coaxial slot at the and face a closed single-mode feed waveguide close to its external wall (Fig. 4: the slot length and width are 1.6 and 0.06, respectively) allows radiating 55% ( $\bar{k} \approx 5.17$ ) to 100% ( $\bar{k} \approx 1.8$ ) of the fed power into free space at frequencies  $\bar{k}$  corresponding to half-wave resonances for the propagational  $TEM$ -mode ( $\bar{\lambda} \approx 3.49; 1.72; 1.21$ ).

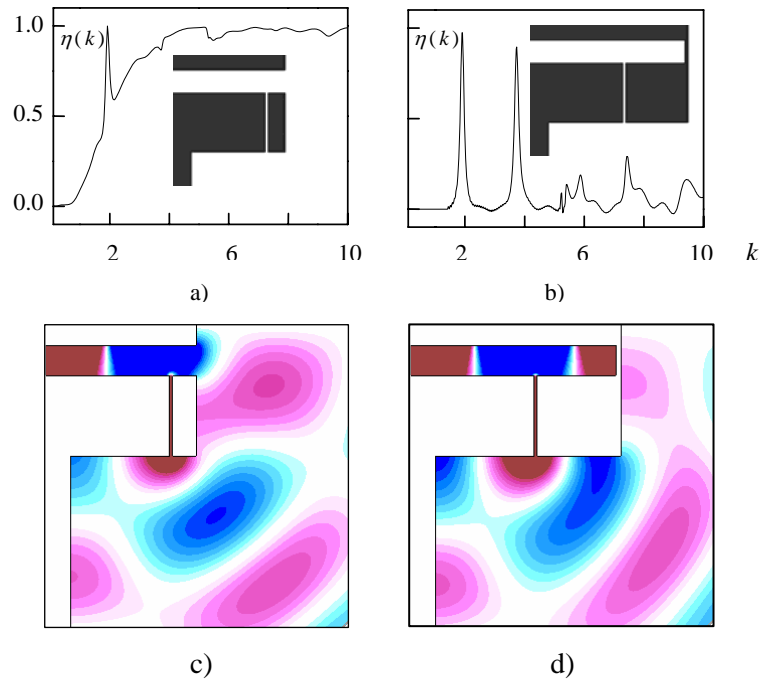


**FIGURE 3.** Narrow radial slots in the external conductor of antenna 1: radiation efficiencies (a) and (b), and spatial distributions (c) and (d) of the  $H_\phi(g,t)$  magnitudes ( $t=70$ ) for the case of radiator excitation by a quasimonochromatic  $TEM$ -mode (Eq.(2)) whose central frequency,  $\bar{k} = 1.91$ , corresponds to the frequency of the first slot resonance

Application of two coaxial slots in antenna 1 (Fig. 5: the slot lengths are equal to 0.76; the widths of the slots at the end-faces of the central and external conductors are 0.18 and 0.12, respectively; the thickness of the partition between the waveguide and the slots is equal to 0.03) makes it possible to change the radiation efficiency,  $\eta(k)$ , within a broad range by varying the parameter  $k$  over a small interval of magnitudes. Specifically, more than 85% of the fed power is radiated within the range  $1.7 < k < 1.82$ , while less than 5% for the range  $1.86 < k < 2.0$ .

The central frequency,  $\bar{k} = 1.85$  ( $\bar{\lambda} \approx 3.4$ ), of the range corresponds to a quarter-wave resonance for the *TEM*-mode in a narrow circular coaxial waveguide.

In the case of a high radiation efficiency the feed line and the slots operate synchronously in phase (the field phases are the same), while in the case of a “blinded” antenna they are in a counter-phase. In the former case the orientation of the main lobe of the antenna pattern ( $\bar{\vartheta} \approx 54^\circ$ ) is nearly the same as for the basic structure. The effect of a sharply changing radiation efficiency is retained when the slot position is changed at the end-face (i.e., the slots are displaced along the  $\rho$ -axis), however the range of variations of  $\eta(k)$  is reduced. The reason is that it becomes more difficult to match the fields in the feed waveguide and the slot resonators.

## SLOT RESONANCES IN ANTENNA 2

When the length of the monopole is equal to about one half of the wavelength or one wavelength of the *TEM*-mode driving the structure (i.e.,  $k \approx 1.25$  or  $k \approx 2.5$ , respectively), the radiation efficiency of antenna 2 reduces to 78 or 95%, respectively. The radiation efficiency can be increased through the use of a quarter-wavelength longitudinal slot at the end-face of the central conductor, as it has been done, for example, in the antenna 1 of Fig. 5. This is the case where the antenna pattern changes only slightly and in a narrow frequency range around the resonance frequency.

A transverse quarter-wavelength slot in the bulge of the central conductor of the feed line (Fig. 6: the width of the slot filled by a dielectric material  $\varepsilon = 4$  is equal to 0.06; the slot length is 0.36; the plane  $z = 0.2$  bisects the slot) allows changing the  $\eta(k)$  function over a wide range of magnitudes by varying the parameter  $k$  within narrow limits. The radiation efficiency can be as high as 98% with  $k \approx 1.27$ , while it drops down to zero for  $k \approx 1.38$ . The antenna



pattern remains practically unchanged (compare Figs. 2(b) and 6(a)), however its main lobe becomes somewhat wider at the maximum value of  $\eta(k)$ .

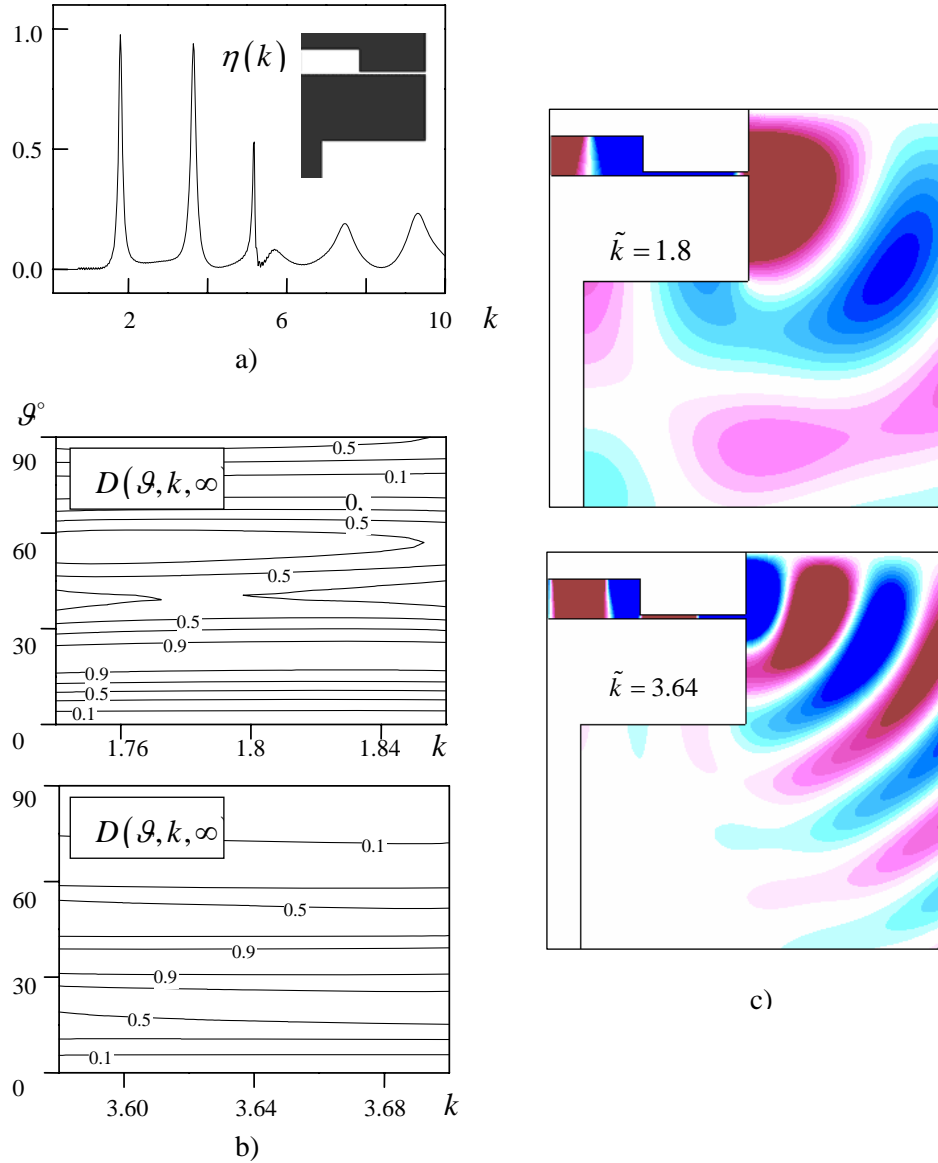
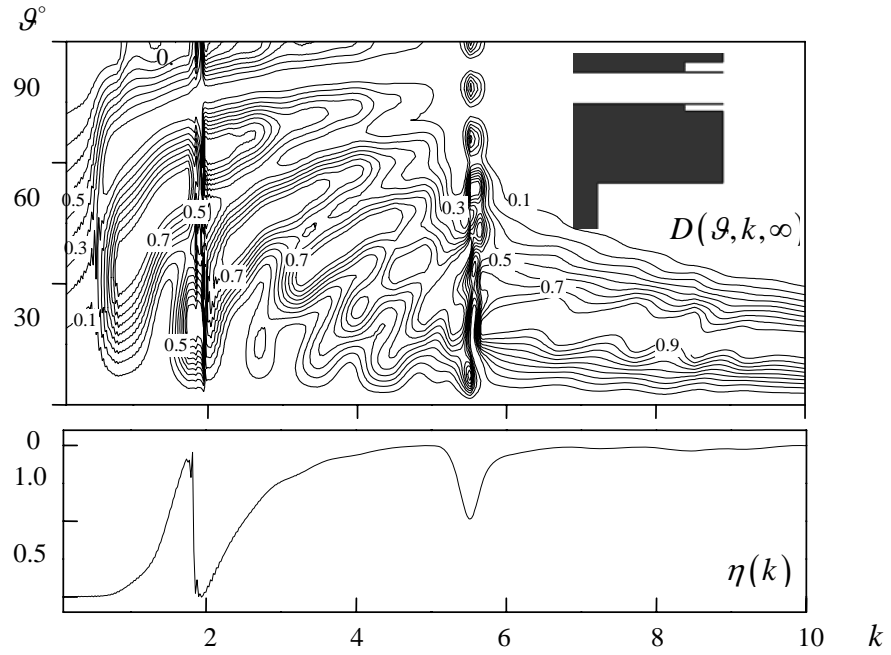
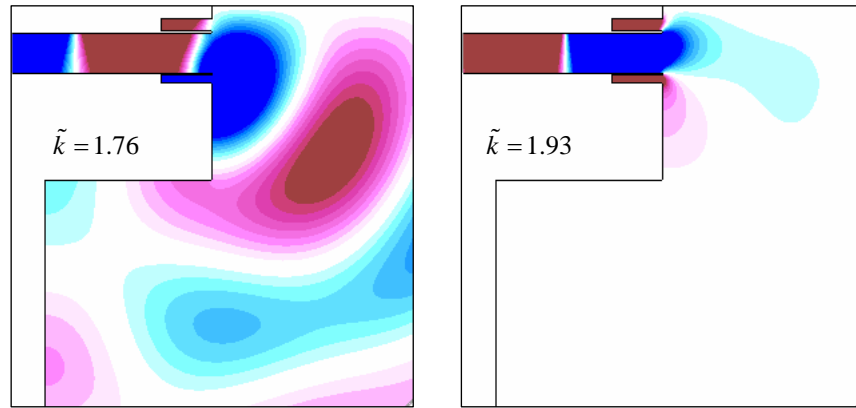


**FIGURE 4.** A narrow coaxial slot at the end-face of the closed feed waveguide: the radiation efficiency over the frequency range considered (a); antenna pattern in the vicinity of the two first maxima of the radiation efficiency (b), and spatial distribution of the  $H_\phi(g, t)$ -magnitudes (with  $t = 70$ ) for the radiator excited by the quasi monochromatic  $TEM$ -mode Eq. (2) (c)

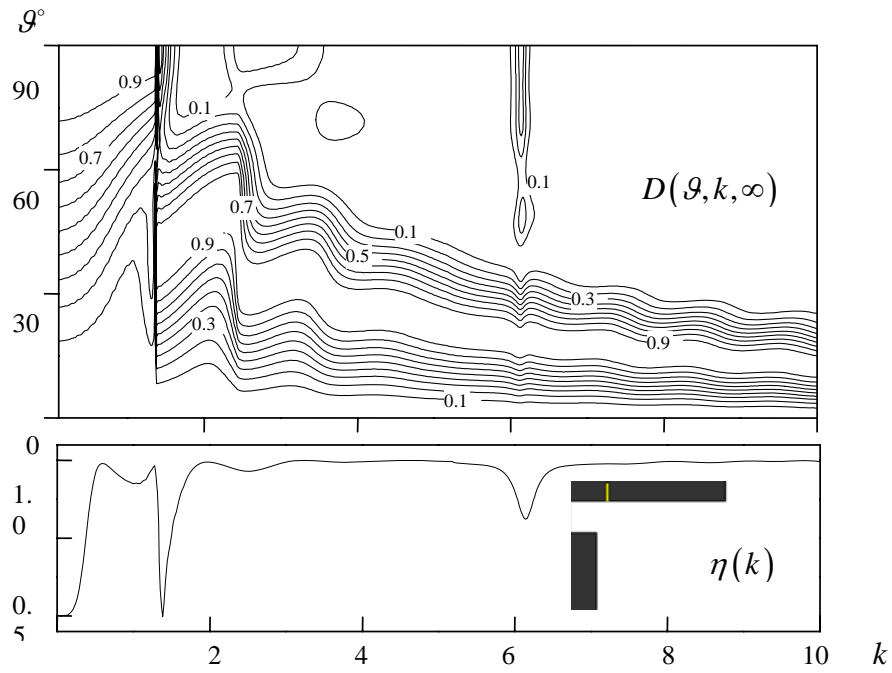


a)

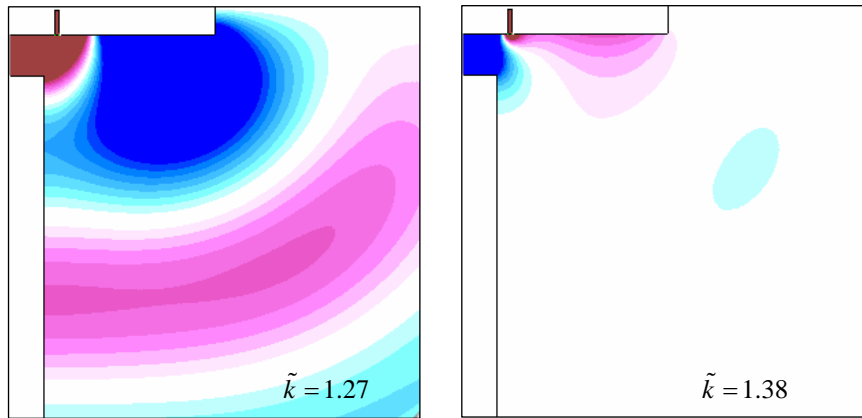


b)

**FIGURE 5.** A coaxial slot at the end-face of the radiating structure: the antenna pattern and radiation efficiency of the radiator over the frequency range considered (a); and spatial distribution of the excited by the  $H_\phi(g, t)$  magnitudes (with  $t=70$ ) for the radiator excited by the quasimonochromatic  $TEM$ -mode Eq. (2) (b)



a)



b)

**FIGURE 6.** A cylindrical monopole with a thin transverse slot filled by a dielectric material with  $\varepsilon = 4$ : the antenna pattern and radiation efficiency of the radiator over the frequency range considered (a), and spatial distribution of the  $H_\phi(g, t)$ -magnitudes (with  $t = 70$ ) for the radiator excited by the quasimonochromatic  $TEM$ -mode given (2) (b)

The slot position with respect to the plane  $z = 0$  is an important parameter to control the basic characteristics of the radiator. Thus, should a similar slot be shifted, for example, along the  $z$ -axis by a distance equal to 1.2, then the radiation efficiency of the antenna would decrease to 35% at  $k \approx 1.28$ , while it would increase to 100% at  $k \approx 1.42$ . With  $1.36 < k < 1.41$  the main lobe of the antenna pattern gets reoriented toward  $\bar{\vartheta} \approx 90^\circ$ , and its 0.5-level width attains the value of  $70^\circ$ .

## CONCLUSIONS

Thus, slot resonances of *TEM*-modes in narrow radial and circular coaxial waveguides allow changing essentially the basic characteristics of axially-symmetric antennas of standard configuration. Several effects have been revealed and analyzed, including i) antenna blinding by resonances in thin transverse and longitudinal short-circuited slot in the external and internal conductors of the coaxial feed line and ii) total transmission of the fed power into free space through narrow slots in the closed end and thick external conductor of the coaxial waveguide. The slot resonances can be used for constructing efficient and simple circuits to control electrodynamic properties of antennas of various kinds and application.

*Acknowledgement.* The author would like to thank Prof. P.N. Melezhik for his constructive criticism in discussing the result obtained, and Dr. V.L. Pazynin for the help in implementing the software of the algorithms.

The work was partially supported by a Young Scientists grant of from the National Academy of Sciences of Ukraine.

## REFERENCES

1. Isom, R., Iskander, M.F., Yun, Z., and Zhang, Z., (2004), Design and development of multiband coaxial continuous transverse stub (CTS) antenna arrays, *IEEE Trans. on AP*. 52(8):2180-2184.
2. Pazynin, V.L. and Sirenko, K.Yu., (2005), Conversion of pulse-modulated  $TM_{0n}$ - and  $TE_{0n}$ -modes by axially-symmetric waveguiding units. Slot resonances, *Elektromagnitnye Wolny i Elektronnye Sistemy*. **10**(10):21-26 (in Russian).
3. Sirenko, Yu.K., Pazynin, V.L., Vyazmitinova, A.I., and Sirenko, K.Yu., (2003), Compact-size irregularities in free-space: virtual boundaries in scalar and vectorial "open", initial and boundary value problem of the theory of scattering for

- nonsinusoidal electromagnetic waves, *Elektromagnitnye Wolny i Elektronnyye Sistemy*. **8**(1-12):33-54 (in Russian).
4. Sirenko, Yu.K., and Sirenko, K.Yu., (2005), Exact “absorbing” conditions in initial and boundary value problems of the theory of open waveguide-based resonator, *Zhurn. Vychisl. Mathem. and Mathem. Fiziki*. **45**(3):509-525 (in Russian).
  5. Taflove, A., (1995), *Computational electrodynamics – the finite difference time domain method*, Massachusetts, Artech House, 599 p.
  6. Pazynin, V.L., and Sirenko, K.Yu., (2005), *A rigorous approach to analyzing transient processes in axially-symmetric waveguiding units*, *Radiofizika i Elektronika*. **10**(2):183-192 (in Russian).
  7. Maloney, J.G., and Smith, G.S., (1993), A study of transient radiation from the Wu-King resistive monopole – FDTD analysis and experimental measurements, *IEEE Trans. on AP*. **41**(5):668-676.